dicted value in **2a** of 1494 cm^{-1}. A smaller scaling factor of 0.860 is required to fit the calculated RHF/3-21G frequency of 1811 cm^{-1} for **2b** to the experimental value[3] of 1557 cm^{-1}. Using this scaling factor, together with the RHF/3-21G value of 1742 cm^{-1} for the C=C stretch in **2a**, gives a predicted frequency of 1498 cm^{-1}.

The close agreement of the scaled frequencies, obtained from two different types of electronic structure calculations, with that of the weak absorption at 1496 cm^{-1} in the IR spectrum of **2a** provides support for assigning this band to the C=C stretch in **2a**. The frequency of this band is about 60 cm^{-1} lower than that of the corresponding stretching frequency in **2b**[3] and about 185 cm^{-1} lower than the frequencies for the C=C stretch in bicyclo[3.3.0]oct-1(5)-ene[16] and in tetramethylethylene. The highly pyramidalized, nearly tetrahedral geometry,[6] to which the doubly bonded carbons in **2a** are constrained by the rigid tricyclic skeleton, obviously has a substantial effect on lowering the C=C stretching frequency from those found in unconstrained alkenes.

Experimental Section

Synthesis of 3,7-Diiodotricyclo[3.3.1.0^{3,7}]nonane.[7] A solution of 200 mg of tricyclo[3.3.1.0^{3,7}]nonane-3,7-diol[17] and 3.0 g of sodium iodide in 10 mL of 95% phosphoric acid was heated at 110 °C for 48 h. The purple reaction mixture was then cooled, diluted with 20 mL of water, and extracted with three 20-mL portions of diethyl ether. The combined ether solutions were washed with two 25-mL portions of saturated, aqueous sodium thiosulfate and 20 mL of saturated, aqueous sodium chloride and then dried over magnesium sulfate. Removal of solvent under vacuum gave a yellow solid, which was chromatographed on 5 g of silical gel, using hexane–ethyl acetate (10:1) to elute the column. Isolated was 195 mg (40%) of the diiodide as a white, crystalline solid, mp 130–131 °C and pure by ^{1}H NMR, after sublimation under vacuum. ^{1}H NMR (500 MHz, $CDCl_3$): δ 2.76 (d, 4 H, J = 10.3 Hz), 2.43 (d, 4 H, J = 10.3 Hz), 1.90 (s, 2 H), 1.63 (s, 2 H). ^{13}C NMR (50 MHz, $CDCl_3$) 57.79 (t), 53.14 (s), 39.45 (d), 30.78 (t). Exact mass. Calcd for $C_9H_{12}I_2$: 373.9028. Found: 373.9036.

Matrix Isolation Procedure. A sample of 3,7-diiodotricyclo-[3.3.1.0^{3,7}]nonane was sublimed at 60 °C into a stream of potassium or cesium vapor, diluted with argon, passed through a 2 in. long hot zone that was heated to 180 °C, and condensed on a CsI window that was maintained at 10 K using an Air Products CS-202 Displex closed-cycle helium cryostat. The IR spectra were obtained with a Nicolet 60-SXR FTIR spectrometer. The photobleaching was performed with the 248-nm KrF line of a Lambda Physik EMG 50E excimer laser.

Calculations. Vibrational analyses, using the semiempirical MNDO method,[18] as well as ab initio RHF calculations with the 3-21G basis set[19] were performed with the package of programs in Gaussian 90.[20]

Acknowledgment. This work was supported by the National Science Foundation (Grants CHE-9020896 and CHE-9016931). Much of the experimental work reported here was performed while J.G.R. and J.M. were at the University of Texas, Austin.

(16) Warner, P.; LaRose, R.; Schleis, T. *Tetrahedron Lett.* **1974**, *15*, 1409. Hrovat, D. A.; Miyake, F.; Trammell, G.; Gilbert, K. E.; Mitchell, J.; Clardy, J.; Borden, W. T. *J. Am. Chem. Soc.* **1987**, *109*, 5524.

(17) Borden, W. T.; Ravindranathan, T. *J. Org. Chem.* **1971**, *36*, 4125. Mori, T.; Kimoto, K. H.; Nozaki, H. *Tetrahedron Lett.* **1970**, *11*, 2419.

(18) Dewar, M. J. S.; Thiel, W. *J. Am. Chem. Soc.* **1977**, *99*, 4899.

(19) Binkley, J. S.; Pople, J. A.; Hehre, W. J. *J. Am. Chem. Soc.* **1980**, *102*, 939.

(20) Frisch, M. J.; Head-Gordon, M.; Trucks, G. W.; Foresman, J. B.; Schlegel, H. B.; Raghavachari, K.; Robb, M.; Binkley, J. S.; Gonzalez, C.; Defrees, D. J.; Fox, D. J.; Whiteside, R. A.; Seeger, R.; Melius, C. F.; Baker, J.; Martin, R. L.; Kahn, L. R.; Stewart, J. J. P.; Topiol, S.; Pople, J. A. Gaussian 90; Gaussian, Inc.: Pittsburgh, PA, 1990.

Slow Amide Proton Exchange Rates from the Line Widths in a Single Two-Dimensional ^{1}H NMR Spectrum

Helle B. Olsen, Henrik Gesmar, and Jens J. Led*

Contribution from the Department of Chemistry, University of Copenhagen, The H. C. Ørsted Institute, Universitetsparken 5, DK-2100 Copenhagen Ø, Denmark. *Received June 8, 1992*

Abstract: A method is presented that allows a quantitative determination of chemical exchange rates of the order of reciprocal hours from the line widths of the signals in a single two-dimensional ^{1}H nuclear magnetic resonance spectrum. The method is based on a linear prediction analysis of the time domain signal and a nonlinear least squares fit of the entire frequency domain signal. The applicability of the method is demonstrated by the determination of the exchange rates of seven slowly exchanging amide protons in the des-[Phe(B25)] mutant of human insulin.

Introduction

The exchange of amide protons in proteins has attracted much attention over the years due to its close relation to the secondary and tertiary structure of the proteins. In particular NMR spectroscopy has proved valuable in such studies since it allows a determination of the rate of exchange of individual amide protons in the range from reciprocal milliseconds to reciprocal months.

In principle, the rate of exchange of relatively slowly exchanging amide protons in proteins can be determined from series of 1D NMR spectra,[1,2] by following the decay of the intensities of the amide proton signals after dissolution of the protein in D_2O. However, in the case of larger peptides and proteins a determination of the rates from 1D NMR spectra is often prevented by signal overlap and line broadening. This resolution problem can be reduced considerably by using series of 2D NMR spectra.[3] Because of the large amount of time necessary to record such series, the NMR measurements are normally carried out independently of the exchange process in order to ensure a sufficient time resolution for this process. Thus, samples corresponding to the individual 2D NMR spectra are removed from a stock solution of the exchanging protein at different time intervals after the start of the exchange, and the exchange process is quenched prior to the NMR experiment. This procedures ensures a time resolution for the exchange process that is independent of the time interval between consecutive 2D NMR spectra in the series. At the same time, however, it makes considerable demands on the amount of protein. Also a calibration of the individual spectra is normally

* Author to whom correspondence should be addressed.

(1) Glickson, J. D.; Phillips, W. D.; Rupley, J. A. *J. Am. Chem. Soc.* **1971**, *93*, 4031-4038.

(2) Richarz, R.; Sehr, P.; Wagner, G.; Wüthrich, K. *J. Mol. Biol.* **1979**, *130*, 19-30.

(3) Wagner, G.; Wüthrich, K. *J. Mol. Biol.* **1982**, *160*, 343-361.

0002-7863/93/1515-1456$04.00/0

necessary in order to ensure compatibility. In cases where quenching is not possible,[4] real-time determinations of the exchange rates have been made by recording the series of 2D NMR spectra during the exchange process. This, however, can be done only at the expense of a reduced time resolution for the exchange process. More recently, a method[5] that alleviates this problem, by reducing the time necessary for recording the 2D NMR spectra, has been proposed. Still, common features of the methods based on series of 2D NMR spectra are the considerable amount of data and of spectrometer time needed and the necessity of calibrating the spectra.

Here we present a method for quantitative determination of the rate of exchange of amide protons that exchange within hours. The experimental data necessary for the determination are limited to a *single* 2D NMR spectrum recorded during the exchange processes. The method exploits the line broadening of the amide proton cross peaks caused by the proton exchange.[6] The determination of these line broadenings is based on detailed linear prediction[7,8] analyses and least squares calculations.[9,10] Although only one 2D NMR spectrum is being used, the method ensures a high time resolution for the exchange process, as well as a high spectral resolution. Furthermore, the use of only one spectrum makes a calibration of the data unnecessary, just as it eases the demand on the amount of sample and of experimental data.

Theory

In the absence of exchange, the decay of the individual resonances in the time domain signal (the free induction decay, FID) obtained in a NMR experiment is given by

$$m(t) \propto \exp(-tR_2^*) \tag{1}$$

assuming that the transverse relaxation in a first-order process with the effective rate constant R_2^*. From the corresponding frequency domain signal is derived the well-known expression[11] for the line width at half height

$$\Delta\nu_{1/2} = \frac{1}{\pi}R_2^* \tag{2}$$

which allows R_2^* to be determined from the line width. If an exchange of protons takes place, as for example in the case of exchange of the amide protons in a protein with deuterium from solvent D_2O, the rate of decay of the corresponding ^1H FID is further increased, that is,

$$m(t,t_{exch}) \propto \exp(-(tR_2^* + t_{exch}k_{exch})) \tag{3}$$

Here k_{exch} and t_{exch} are the first-order rate constant and the time, respectively, for the exchange process.

In eq 3 the parameters t and t_{exch} refer to the same time scale. However, in the case of t_1 FIDs in a 2D NMR experiment, the R_2 relaxation and the exchange process refer to different time scales. The relaxation refers to the time scale of the evolution time, t_1, of the 2D experiment, while the exchange process progresses on a real-time scale. Thus, as far as the relaxation is concerned, the time difference between consecutive data points in the t_1 FID is given by the increment of the evolution time, Δt_1, whereas in the case of the exchange process, it is given by the difference in real time between the start of two consecutive t_2 FIDs, Δt_{exch}. Therefore, for a suitable exchange rate the condition $k_{exch}\Delta t_{exch} \simeq R_2^*\Delta t_1$ will be fulfilled, and similar decays in the two different processes will be followed during the 2D NMR experiment.

In the specific case of the ^1H NOESY experiment, the FID intensity expressed as a function of t_1, τ_m, t_2, and t_{exch} is given by a modified version of eq 9.3.12 in ref 12:

$$\mathbf{M}^+(t_1,\tau_m,t_2,t_{exch}) = -\exp\{\mathbf{L}^+t_2\}\exp\{\mathbf{L}\tau_m\}\exp\{\mathbf{L}^+t_1\}\exp\{\mathbf{K}_{exch}t_{exch}\}\mathbf{M}_0 \tag{4}$$

where $\mathbf{M}^+ = \mathbf{M}_x + \mathcal{J}\mathbf{M}_y$, $\mathbf{L}^+ = \mathcal{J}\Omega - \Lambda - \mathbf{K}_{exch}$, $\mathbf{L} = -\mathbf{R} - \mathbf{K}_{exch}$, τ_m is the mixing time, and $\mathbf{M}_0 = \mathbf{M}^+(0,0,0,0)$. The diagonal matrices Ω, Λ, and $\mathbf{K}_{exch}$ contain the chemical shifts, Ω_j, the transverse relaxation rates, R_{2j}^*, and the first-order rate constants, $k_{exch,j}$, respectively. The matrix $\mathbf{K}_{exch}$ is diagonal as only exchange with solvent deuterium is considered here. The original kinetic matrix $\mathbf{K}$ in ref 12 is omitted as no intramolecular chemical exchange was included in the analysis. The nondiagonal matrix $\mathbf{R}$ contains the longitudinal and cross relaxation rates. $\mathcal{J}$ is the imaginary unit. Equation 4 is valid only for the case of unresolved scalar couplings. If the FIDs are sampled by signal averaging, the right-hand side of eq 4 should be scaled by a diagonal matrix $\mathbf{S}$, the ith element of which is $(1 - \exp(-k_{exch,i}\Delta t_{exch}))/(1 - \exp(-k_{exch,i}\Delta t_r))$, where Δt_r is the repetition time between the individual scans. This, however, has no influence on the line width.

Since the value of t_1 is incremented at regular time intervals, Δt_{exch}, during the 2D experiment, $t_{exch}/t_1 = \Delta t_{exch}/\Delta t_1$, and eq 4 can be recast as

$$\mathbf{M}^+(t_1,\tau_m,t_2,t_{exch}) = -\mathbf{S}\exp\{\mathbf{L}^+t_2\}\exp\{\mathbf{L}\tau_m\}\exp\{(\mathbf{L}^+ + \mathbf{K}_{exch}\Delta t_{exch}/\Delta t_1)t_1\}\mathbf{M}_0 \tag{5}$$

The line width along F_1 of the cross peak at (Ω_i,Ω_j) is therefore given by $^1\Delta\nu_{1/2,j} = (R_{2j}^* + k_{exch,j}\Delta t_{exch}/\Delta t_1)/\pi$, while the line width of the "mirror image" at (Ω_j,Ω_i) along F_2 is given by $^2\Delta\nu_{1/2,j} = (R_{2j}^* + k_{exch,j})/\pi$. Thus

$$^1\Delta\nu_{1/2,j} - {}^2\Delta\nu_{1/2,j} = (k_{exch,j}\Delta t_{exch}/\Delta t_1)/\pi \tag{6}$$

i.e.,

$$k_{exch,j} = \pi({}^1\Delta\nu_{1/2,j} - {}^2\Delta\nu_{1/2,j})(\Delta t_1/\Delta t_{exch}) \tag{7}$$

Typical values for Δt_1 and Δt_{exch} used in 2D NMR experiments are 25–50 μs and 100 s, respectively. Consequently, exchange processes that are of the order of 10^5–10^6 times slower than the relaxation will affect the decay of the t_1 FID. This implies that exchange processes that are completed on the order of hours, i.e., during a 2D NMR experiment, will give rise to measurable broadenings of the signals in the F_1 dimension. The exchange rate can be calculated from eq 7, using the F_1 and F_2 line widths from the same 2D NMR spectrum.

Despite the simplicity of this method, it has, so far, not been applied due to difficulties in obtaining accurate line widths from 2D ^1H NMR spectra of peptides and proteins. However, recent developments in linear prediction[7] (LP) and least squares[9,10] (LSQ) analyses of complicated NMR spectra have greatly improved the possibility of retrieving quantitative spectral information in such cases. Thus, a LP analysis of the FID can provide estimates of the four parameters that describe each one of the signals in the spectrum, i.e., the frequency, the line width, the intensity, and the phase. By using these estimates as starting parameters in a LSQ analysis of the entire frequency domain signal, one can retrieve the maximum information contained in the experimental NMR data, provided the analysis is based on the complete analytical expression for the discrete Fourier transform of a sum of exponentially decaying signals;[10] that is

$$S(\nu) = \sum_{j=1}^{p} A_j \frac{1 - \exp(\mathcal{J}2\pi(\nu_j - \nu) - R_{2j}T_{aq})}{1 - \exp(\mathcal{J}2\pi(\nu_j - \nu) - R_{2j}/SW)} \tag{8}$$

Here $A_j = I_j \exp((\mathcal{J}2\pi\nu_j - R_{2j})T_{in} + \mathcal{J}\phi_j)$, and I_j, ν_j, R_{2j}, and ϕ_j are the intensity, the frequency, the relaxation rate, and the phase, respectively, of the jth signal. T_{in} is the initial delay, T_{aq}

(4) Boelens, R.; Gros, P.; Scheek, R. M.; Verpoorte, J. A.; Kaptein, R. *J. Biomol. Struct. Dyn.* **1985**, *3*(2), 269–280.
(5) Mariõn, D.; Ikura, M.; Tschudin, R.; Bax, A. *J. Magn. Reson.* **1989**, *85*, 393–399.
(6) Labhardt, A. M.; Hunziker-Kvik, E.-H.; Wüthrich, K. *Eur. J. Biochem.* **1988**, *177*, 295–305.
(7) Gesmar, H.; Led, J. J. *J. Magn. Reson.* **1988**, *76*, 183–192.
(8) Led, J. J.; Gesmar, H. *Chem. Rev.* **1991**, *91*, 1413–1426.
(9) Abildgaard, F.; Gesmar, H.; Led, J. J. *J. Magn. Reson.* **1988**, *79*, 78–89.
(10) Gesmar, H.; Led, J. J.; Abildgaard, F. *Prog. Nucl. Magn. Reson. Spectrosc.* **1990**, *22*, 255–288.
(11) Becker, E. D. *High Resolution NMR*, 2nd ed.; Academic Press, Inc: New York, 1980, pp 184–197.
(12) Ernst, R. R.; Bodenhausen, G.; Wokaun, A. *Principles of Nuclear Magnetic Resonance in One and Two Dimensions*; Clarendon Press: Oxford, 1987; p 498.

is the acquisition time, and SW is the sweep width.

Experimental Section

Lyophilized des-[Phe(B25)] human insulin, made by use of DNA technology and purified as described previously,[13] was dissolved in D_2O at pH 3.0 to a concentration of 5 mM. No buffer was used. The sample was placed in a 5-mm NMR tube, and the spectra were recorded at 310 K on a Bruker AM500 NMR spectrometer equipped with an ASPECT 3000 computer. The data acquisition was started as soon as possible (≤20 min) after the dissolution. The ^1H NOESY spectra[14] were recorded with a mixing time of 150 ms. The FIDs consisted of 8192 data points in the t_2 dimension and 2047 in the t_1 dimension. The spectra were recorded with sequential quadrature detection in the t_2 dimension[15] and time proportional phase increment (TPPI) in the t_1 dimension.[16-18] A large sweep width (20 000 Hz) was used in both dimensions in order to reduce base-line distortion due to aliasing caused by zoning.[9,19]

The experimental data were processed on a VAX 6410 computer and displayed on VAXstations, using locally developed software. The LP and LSQ analyses were performed using vectorized versions of the programs NMRFIT and LPEXTRAPOL. A modified version of a recently developed Toeplitz algorithm[20] was used for the LP calculations. Before the LP analysis of the FIDs in one of the two dimensions (the active dimension), the FIDs in the other dimension (the passive dimension) were zero-field to twice the number of data points, multiplied by a window function, and Fourier transformed. In the t_2 dimension the applied window function was a $\pi/2$-shifted sinebell together with a convolution difference with a line broadening of 20 Hz and a scaling factor of 0.5. In the t_1 dimension the same convolution difference was used together with a trapezoidal filter ranging from data point 512 to the end of the FID. Finally, phase correction was applied to the passive dimension.

The LSQ analysis of the frequency domain data was based on the frequencies and line widths found by the LP analysis. Before the Fourier transformation, the FIDs were zero-filled to twice the number of data points. No window multiplications or phase correction was used in this case. Initially, a linear LSQ analysis was performed in which the phases and intensities of the signals were determined, while the frequencies and the line widths were fixed at the values obtained in the LP analysis. Subsequently, an iterative nonlinear LSQ fit was performed in which all four parameters for the signals in the slice were adjusted simultaneously. In both types of LSQ analyses eq 8 was applied. In order to improve the accuracy of the parameters, the LSQ fits were made using sums of slices in the 2D NMR spectrum; that is, several slices containing the signals to be analyzed were added before the analysis.

The time used for a complete analysis of a single cross peak was approximately 5 h using the VAX 6410 computer. The computation included a LP calculation with 800 LP coefficients in the t_1 dimension and 3096 coefficients in the t_2 dimension followed by the linear and nonlinear LSQ analyses of the frequency domain signals described above. Due to the efficiency of the Toeplitz algorithm used in the determination of the LP coefficients and the fact that these calculations are well suited for vectorization, this part of the computation took less than 1% of the entire computation time, while the rest of the time was consumed by the LSQ analyses. With more recently developed minicomputers than the one used here, the total amount of computation time can easily be reduced by an order of magnitude.

Results and Discussion

The proposed method was applied in the study of the 50-residue des-[Phe(B25)] mutant of human insulin. A complete assignment of the NMR spectrum of the mutant will be published elsewhere. In this mutant all but 10 amide protons exchange almost immediately after insulin dissolution, while the exchange of the remaining 10 amide protons was completed within 24 h under the experimental conditions applied here. The slowly exchanging amide protons are mainly located in regions of the peptide chain

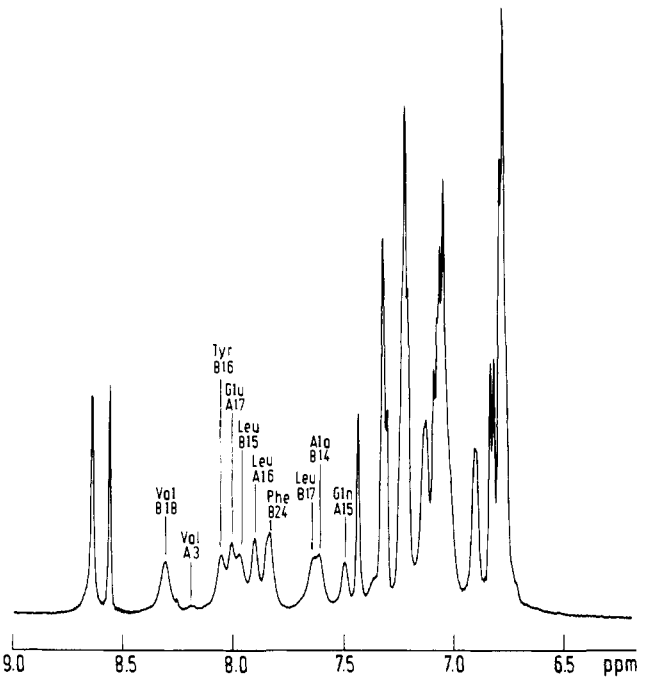

Figure 1. The amide proton region of the 500-MHz ^1H NMR spectrum of a 5 mM solution of the des-[Phe(B25)] mutant of human insulin at 310 K and pH 3.0. The spectrum was recorded 20 min after dissolution of the protein in D_2O.

where helix structure is observed in a series of other closely related insulin mutants.[13,21-23]

Figure 1 shows the amide aromatic regions of the 1D NMR spectrum of des-[Phe(B25)] insulin immediately after dissolution of the protium-containing protein in D_2O. The spectrum is characterized by broad and overlapping NH signals that are difficult to separate. Expansion of the spectrum into two dimensions alleviates this problem. Figure 2 shows part of a NOESY spectrum sampled during the exchange process. Unlike the procedure followed in the LSQ analyses where any manipulation of the data was omitted, the appearance of the spectrum in Figure 2 was improved by window multiplication and phase correction. The contour plot in Figure 2 shows a number of cross peaks correlating the slowly exchanging amide protons with nonexchanging protons in the side chain of the same residue, or in the side chains of neighboring residues. Evidently, the exchange gives rise to a considerable line broadening of these cross peaks in the F_1 dimension, whereas it has no effect on the line widths in the F_2 dimension. Referring to eq 7, $^1\Delta\nu_{1/2}$ is the line width of the cross peak in the F_1 dimension below the diagonal, whereas $^2\Delta\nu_{1/2}$ is the line width of the symmetric cross peak in the F_2 dimension above the diagonal. The possibility of making a second, independent determination of the exchange rates, using $^1\Delta\nu_{1/2}$ from the cross peak above the diagonal and $^2\Delta\nu_{1/2}$ from the cross peak below the diagonal, is hampered by the passive couplings that affect these line widths. Also, use of the diagonal NH peaks in the 2D spectrum is prevented by severe signal overlaps.

The quality of the fit is illustrated in Figure 3, which shows slices along the two dimensions in the spectrum in Figure 2. The slices go through the NH–γCH_3 cross peak of Val(B18). Both the experimental slices and the slices calculated from the parameters obtained by the combined LP/LSQ analysis are shown. The excellent accordance between the experimental and calculated slices is indicated by their difference, also given in Figure 3. The same accordance is evident from the relatively small errors on the calculated line widths given in Table I.

(13) Kristensen, S. M.; Jørgensen, A. M. M.; Led, J. J.; Balschmidt, P.; Hansen, F. B. *J. Mol. Biol.* **1991**, *218*, 221–231.
(14) Jeener, J.; Meier, B. H.; Bachmann, P.; Ernst, R. R. *J. Chem. Phys.* **1979**, *71*, 4546–4553.
(15) Redfield, A. G.; Kunz, S. D. *J. Magn. Reson.* **1975**, *19*, 250–254.
(16) Drobny, G.; Pines, A.; Sinton, S.; Weitekamp, D. P.; Wemmer, D. *Faraday Div. Chem. Soc. Symp.* **1979**, *13*, 49–55.
(17) Bodenhausen, G.; Vold, R. L.; Vold, R. R. *J. Magn. Reson.* **1980**, *37*, 93–106.
(18) Marion, D.; Wüthrich, K. *Biochem. Biophys. Res. Commun.* **1983**, *113*, 967–974.
(19) Hoult, D. I.; Richards, R. E. *Proc. R. Soc. London* **1975**, *A344*, 311–320.
(20) Cybenko, G. *SIAM J. Sci. Stat. Comput.* **1987**, *8*, 734–740.
(21) Boelens, R.; Ganadu, M. L.; Verheyden, P.; Kaptein, R. *Eur. J. Biochem.* **1990**, *191*, 147–153.
(22) Hua, Q. X.; Shoelson, S. E.; Kochoyan, M.; Weiss, M. A. *Nature* **1991**, *354*, 238–241.
(23) Kline, A. D.; Justice, R. M., Jr. *Biochemistry* **1990**, *29*, 2906–2913.

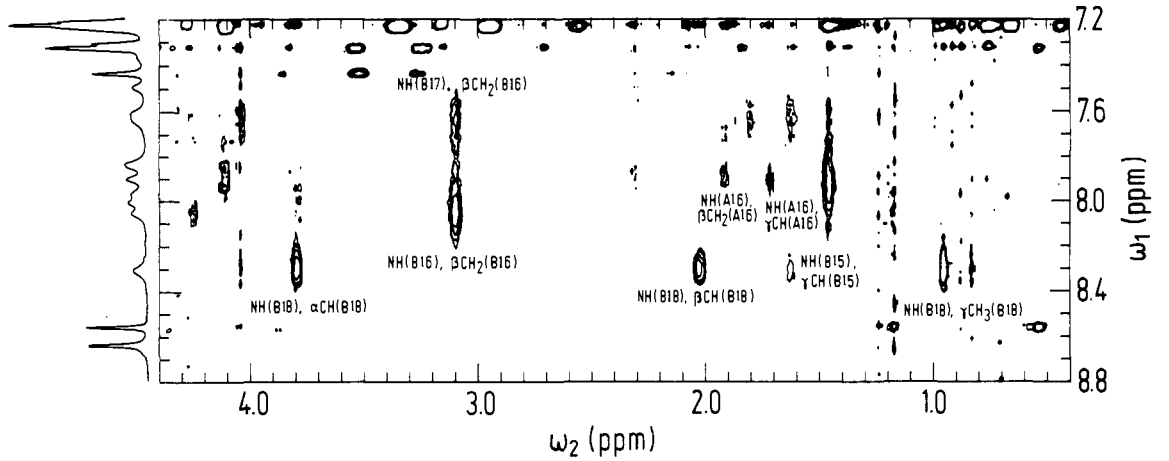

Figure 2. Part of the NOESY spectrum of a 5 mM solution of the des-[Phe(B25)] mutant of human insulin in D_2O obtained at 310 K and pH 3.0. Only the amide correlations below the diagonal of the spectrum are shown. The spectrum was recorded during the exchange of the amide protons. The duration of the experiment was 51 h. The applied window function is described in the Experimental Section.

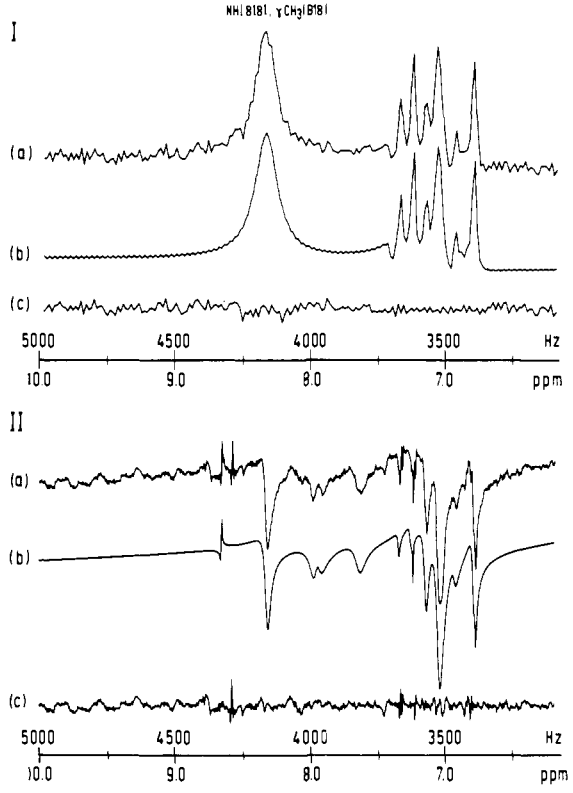

Figure 3. Examples of LSQ analyses in the frequency domain. (I) Sum of five F_1 slices through the NH–γCH_3 cross peak of Val(B18) in the NOESY spectrum shown in Figure 2. (II) Sum of seven F_2 slices through the corresponding NH–γCH_3 cross peak of Val(B18) above the diagonal. In both cases, spectrum a is the experimental spectrum, spectrum b is the spectrum calculated from the parameters obtained by a LSQ analysis (see text) of the experimental spectrum, and spectrum c is the difference between a and b. No phase correction was applied.

In Table I are listed the results for all cross peaks that were analyzed, while in Figure 2 those cross peaks that have intensities above the lowest contour level used in the figure are labeled. As shown in Table I, the accuracy of the exchange rates determined by the method is high. Thus only a few of the exchange rates have 1σ standard deviations above 10%. Moreover, in three cases, namely, Leu(A16), Leu(B17), and Val(B18), where the same exchange rate could be determined independently from different cross peaks, the obtained values agree well within the uncertainties, demonstrating the internal consistency of the method.

The range of exchange rates covered by the method can be further expanded by varying the time of the NMR experiment. Thus, a reduction of the experimental time, obtained by decreasing the number of scans accumulated for each t_1 value, results in a reduction of the exchange broadening, thereby allowing faster exchange rates to be determined. This was demonstrated by recording a NOESY experiment (not shown) with only half the number of scans used for the spectrum in Figure 2, thereby reducing the experimental time from 51 to 26 h. The new spectrum allows a determination of the exchange rate for the relatively fast exchanging Gln(A15) amide proton, as shown in Table I. At the same time the close agreement between the rates obtained from both spectra further demonstrates the reproducibility of the determinations.

Only the amide protons of the three residues Val(A3), Glu(A17), and Ala(B14) exchange too fast (within 2–3 h) to be determined from the NOESY spectra obtained here; i.e., the exchange broadening is too large for the cross peaks to be seen above the noise level in the spectra. Thus, the NH signal from the Val(A3) proton has already lost more than 90% of its intensity after 20 min, corresponding to an exchange rate faster than 15

Table I. Exchange Rate Parameters for Slowly Exchanging Amide Protons[a,b] in des-[Phe(B25)] Human Insulin

NH	correlated to	$^1\Delta\nu_{1/2}$, Hz	$^2\Delta\nu_{1/2}$, Hz	k_{exch}, h^{-1}
		Experimental Time 51 h		
Leu(A16)	βCH_2(A16)	108.0 ± 10.0	16.1 ± 0.7	0.290 ± 0.032
	γCH(A16)	109.0 ± 4.0	29.1 ± 1.1	0.252 ± 0.013
Leu(B15)	γCH(B15)	219.0 ± 6.0	38.0 ± 6.0	0.571 ± 0.027
Tyr(B16)	βCH_2(B16)	139.0 ± 3.0	25.1 ± 1.8	0.359 ± 0.011
Leu(B17)	αCH(B17)	142.0 ± 13.0	30.2 ± 1.8	0.352 ± 0.041
	βCH_2(B16)	152.0 ± 6.0	33.7 ± 1.7	0.373 ± 0.020
Val(B18)	αCH(B18)	90.0 ± 5.0	24.6 ± 1.8	0.206 ± 0.017
	βCH(B18)	85.0 ± 3.0	24.5 ± 0.5	0.191 ± 0.010
	γCH_3(B18)	100.0 ± 3.0	23.7 ± 0.6	0.241 ± 0.010
Phe(B24)	βCH_2(B24)	164.0 ± 12.0	18.7 ± 0.8	0.458 ± 0.038
		Experimental Time 26 h		
Gln(A15)	βCH_2(A15)	183.0 ± 9.0	16.5 ± 1.0	1.032 ± 0.056
Leu(A16)	βCH_2(A16)	76.0 ± 8.0	15.9 ± 1.5	0.373 ± 0.050
	γCH(A16)	72.0 ± 3.0	15.5 ± 0.5	0.350 ± 0.019
Leu(B15)	γCH(B15)	132.0 ± 2.0	41.0 ± 6.0	0.564 ± 0.039
Tyr(B16)	βCH_2(B16)	89.3 ± 1.8	24.9 ± 1.5	0.399 ± 0.015
Leu(B17)	βCH_2(B17)	81.0 ± 13.0	31.0 ± 3.0	0.310 ± 0.083
	βCH_2(B16)	84.0 ± 3.0	30.4 ± 1.9	0.332 ± 0.022
Val(B18)	αCH(B18)	58.0 ± 3.0	22.8 ± 0.4	0.218 ± 0.019
	γCH_3(B18)	58.0 ± 1.9	24.0 ± 3.0	0.211 ± 0.022
	βCH_2(B17)	61.0 ± 3.0	27.0 ± 3.0	0.211 ± 0.026
Phe(B24)	βCH_2(B24)	99.0 ± 6.0	17.0 ± 2.0	0.508 ± 0.039

[a] Including 1σ standard deviations. [b] Obtained at 310 K and pH 3.0. The data were obtained from the analyses of two NOESY spectra with different experimental times. Recording was started 20 min after dissolution of the protium-containing insulin in D_2O. The amide protons in question and their correlation partners are listed in the first two columns. $^1\Delta\nu_{1/2}$ is the line width of the cross peak below the diagonal in the F_1 dimension, and $^2\Delta\nu_{1/2}$ is the line width in the F_2 dimension of the symmetric cross peak above the diagonal.

$h.^{-1}$ The exchanges of the Glu(A17) and Ala(B14) amide protons are somewhat slower, but are still too fast to allow the cross peaks to be observed under the applied experimental conditions.

As discussed above, the internal consistency of the exchange rates determined by the method is demonstrated by the close agreement between the rates obtained from different cross peaks that are influenced by the same exchange process. Also, the reproducibility of the method is evidenced by the accordance between the two experiments in Table I. Still, the compatibility of the rates determined by the method described here and by classical methods[1-3] remains to be established. To that end, the exchange rates of the amide protons of the Val(B18) and Gln(A15) residues, both of which have NH signals with no or little overlap (cf. Figure 1), were determined by monitoring the decays of the two NH signals in a series of 1D spectra recorded immediately after dissolution of the des-[Phe(B25)] insulin in D_2O. The experiment was carried out at pH 3.5 and 310 K, using a 5 mM solution. Although this pH value was slightly higher than the pH value (3.0) of the sample used in the 2D experiment, both values are close to the pH that corresponds to the minimum of the exchange rate of peptide-group hydrogens.[24] Accordingly, the NH exchange rates of 0.234 ± 0.003 and 2.27 ± 0.03 h^{-1}, obtained for Val(B18) and Gln(A15), respectively, from the series of 1D spectra, are both in close agreement with the values obtained in the 2D experiment (cf. Table I). The fact that the 1D value in the case of Val(B18) is the same as the corresponding 2D value within the uncertainty, while it is about a factor of 2 larger in the case of Gln(A15), shows that the pH value for the minimum of the exchange rate of the Gln(A15) NH is lower than that of Val(B18). According to the rules of Molday et al.,[24] this difference in minima is in qualitative agreement with the difference in the primary structure around the two residues.

Finally it should be noted that the range covered by the proposed method can be expanded to include exchange rates slower than those determined here, by increasing the time of the experiment through an increase of the number of scans per t_1 value, or by increasing the sweep width in the F_1 dimension. Thus, for a given R_2^* rate and a given number of experimental data points in the t_1 dimension, an increase of the F_1 sweep width decreases the relaxation decay monitored during a given experimental time, whereas the decay of the FID caused by the exchange remains unaffected. Consequently, for a given relaxation rate, slower exchange processes will affect the FID and can be monitored.

(24) Molday, R. S.; Engelander, S. W.; Kallen, R. G. *Biochemistry* **1972**, *11*, 150-158.

Conclusion

It has been demonstrated that the method presented here allows a quantitative determination of amide proton exchange rates of the order of reciprocal hours. Designing the experimental conditions to the expected exchange rates makes it possible to cover a wider range of rates. Thus the upper limit for the exchange rates covered by the method can be raised by reducing the time of the experiment as demonstrated here, and a combination of this method with the method[5] for fast recording of 2D NMR spectra could possibly extend the range to cover exchange rates of the order of reciprocal minutes. The lower limit for the exchange rates covered by the method is given by the R_2^* relaxation rate and the sweep width in the F_1 dimension and can, in principle, be regulated by adjusting the sweep width.

The applied linear prediction program, LPEXTRAPOL, which is capable of handling TPPI data, and the applied LSQ program, NMRFIT, both written in VAX/VMS FORTRAN, can be obtained from the authors by request.

Acknowledgment. This work was supported by the Danish Technical Research Council, J. No. 16-4679.H, the Danish Natural Science Research Council, J. No. 11-8977-1 and 16-5027, the Ministry of Industry, J. No. 85886, Direktør Ib Henriksens Fond, and Julie Damms Studiefond. We also thank Dr. Per Balschmidt Novo Nordisk A/S for providing the des-[Phe(B25)] insulin.

Conformational Analysis of Six-Membered Rings in Solution: Ring Puckering Coordinates Derived from Vicinal NMR Proton-Proton Coupling Constants

C. A. G. Haasnoot

Contribution from the Department of Analytical Chemistry, Scientific Development Group, Organon International B.V., P.O. Box 20, 5340 BH Oss, The Netherlands.
Received July 20, 1992

Abstract: A new method for quantitative analysis of the conformation of six-membered ring compounds in solution is presented. The method uses as a probe the endocyclic vicinal NMR proton-proton coupling constants, which are translated into the relevant conformational parameters by means of a combination of the generalized Karplus equation and the recently developed Truncated Fourier formalism (delineating the interrelation between the endocyclic torsion angles in a six-membered ring; cf.: Haasnoot, C. A. G. *J. Am. Chem. Soc.* **1992**, *114*, 882). A practical elaboration is laid down in three computational procedures which can be used to analyze the experimental couplings in terms of a single-state conformation or a two-state conformational equilibrium. Typical applications of these procedures are exemplified by conformational analyses of six-membered rings occurring in alkaloids, steroids, and sugar derivatives. The obtained conformational descriptions of these six-membered rings in solution are shown to be consistent with conformational data derived from X-ray crystallography and/or molecular mechanics. It is, therefore, concluded that the unique quantitativeness of the method allows for a superior analysis of the conformational behavior of six-membered rings in solution.

Introduction

Nuclear magnetic resonance (NMR) plays an important role in the conformational analysis of (bio-)(macro-)molecules in solution. One of the pillars of its success is the widespread application of proton-proton coupling constants to conformational problems. A long-standing and rather straightforward example of such an application in the field of six-membered ring systems is the determination of the equilibrium between rapidly exchanging

0002-7863/93/1515-1460$04.00/0